Arab J Geosci (2013) 6:1799–1806
DOI 10.1007/s12517-011-0501-6

ORIGINAL PAPER

Identification and mapping of some soil types using field spectrometry and spectral mixture analyses: a case study of North Sinai, Egypt

A. M. Saleh · A. B. Belal · S. M. Arafat

Received: 27 August 2011 / Accepted: 2 December 2011 / Published online: 22 December 2011

Abstract This study examines linear spectral unmixing technique for mapping the surface soil types using field spectroscopy data as the reference spectra. The investigated area is located in North Sinai, Egypt. The study employed data from the Landsat 7 ETM+ satellite sensor with improved spatial and spectral resolution. Mixed remotely sensed image pixels may lead to inaccurate classification results in most conventional image classification algorithms. Spectral unmixing may solve this problem by resolving those into separate components. Four soil type end-members were identified with minimum noise fraction and pixel purity index analyses. The identified soil types are calcareous soils, dry sabkhas, wet sabkhas, and sand dunes. Soil end-member reference spectra were collected in the field using an ASD FieldSpec Pro spectrometer. Constrained sum-to-one and non-negativity linear spectral unmixing model was applied and the soil types map was produced. The results showed that linear spectral unmixing model can be a useful tool for mapping soil types from ETM+ images.

Keywords Soil mapping · Field spectrometry · Spectral mixture analyses · North Sinai Egypt

Introduction

Soil is one of the most valuable resources. Information from soil and land resource survey is necessary for better management and wise soil use. Soil inventory is often carried out as part of a regional planning and development process in order to determine the location and extent of various soil types and variables. The spatial and temporal variability of surface processes makes soil properties variable and, therefore, makes it difficult to measure directly from their reflectance spectra even under controlled laboratory conditions (Ben-Dor and Banin 1994). Unlike vegetation spectra, the shape of reflectance spectra obtained from soils are mainly invariant in the spectral regions (0.4–1.2 μm; Clark 1999). This may be due to a combined effect of different factors that can affect surface spectral reflectance of soils and make it non-consistent through the spectrum region.

The reflectance from an image pixel is a mixture of the individual reflectance spectra of surface materials (Adams et al. 1986; Smith et al. 1990; Roberts et al. 1993). Spectral mixing occurs when materials with different spectral properties are represented by a single image pixel. Each image pixel contains a spectrum of reflectance values for all the wavebands in the imagery. These spectra may be considered as the signatures of the ground materials such as soil types, provided that the material occupies the whole pixel. Each pixel retains the characteristic features of the individual spectra from each of the component reflective materials.

Spectral unmixing of satellite images is one of the most widely used methods for deriving information from mixed pixels (Lu et al. 2003). Spectral mixture analyses (SMA) are generally defined as the calculation of land cover area fraction within a pixel (Roberts et al. 1998). Spectral mixture analysis was developed for interpreting high spectral resolution advanced visible/infrared images data and was later expanded to be used with Landsat data (Lunetta 1998). The process involves the selection of representative pure spectra (end-member) and the unmixing of the spectral information of a pixel. To get more information from a single pixel, the proportions of these materials can be approximated using a spectral mixing model (Boardman 1994). The spectrum recorded in every image pixel is a linear combination

A. M. Saleh (✉) · A. B. Belal · S. M. Arafat
Soil Sciences Department, National Authority for Remote Sensing and Space Sciences (NARSS),
Cairo, Egypt
e-mail: ahmed_ms@hotmail.com

of a mixture of different components (end-member spectra; Tompkins et al. 1997). Therefore, the value of a pixel in an image for a band equals the weighted sum of the radiance values for that band of all targets present in the pixel (Weng et al. 2004). The linear spectral unmixing model has the following form:

$$R_i = \sum_{k=1}^{n} f_k R_{ik} + E_{Ri}$$

where i the number of spectral bands (1,…,m), k is the number of end-members (1,…, n), R_i is the value of a pixel in band i, f_k is the fraction of end-member k in that pixel, R_{ik} is the radiance of end-member k in band i, and E_{Ri} is the unmodelled residual in band i.

For constrained linear spectral unmixing, the end-member fractions in a pixel are constrained to sum to unity, and each end-member fraction itself is expected not to have a negative value or be greater than 1:

$$\sum_{k=1}^{n} f_k = 1 \text{ and } 0 \le f_k \le 1$$

Unconstrained and constrained unmixing can result in negative abundance values and values greater than 1 for any end-member. The mixing fractions can be determined from the data. For a given number of spectral bands n, an exact solution can be found for each pixel for the unconstrained model if $m=n$ and for the constrained model if $m=n+1$. However, if $m<n$ for unconstrained unmixing or if $m<n+1$ for constrained unmixing, then a least squares fitting procedure can be applied to obtain the best fit.

The model root mean square (RMS) error based on the residuals is

$$\text{RMS} = \sqrt{\sum_{i=1}^{m} (ER_i^2)/m}$$

End-members used for spectral unmixing can be derived from the image itself (called image end-members) or measured in field conditions (reference spectra; Lunetta 1998). Image end-members should be selected from the extreme values of the image spectral feature space representing spectrally the purest pixels (Roberts et al. 1998). As the end-member spectra identified, spectral unmixing of individual pixels can estimate the fractional component spectra and, in turn, the physical fractional component of the materials within the pixels (Adams et al. 1986; Roberts et al. 1993; Theseira et al. 2003). The outputs of linear spectral unmixing are suite of abundance images, one for each end-member in the model. Each abundance image shows the spatial distribution of the spectrally defined material. The aim of this work was to identify and discriminate surface soil types applying linear spectral unmixing technique and field spectroscopy data as the reference spectra under arid conditions.

Materials and methods

Description of the investigated area

The investigated area is located in North Sinai, between 32° 40′ and 34°10′ E and 30°53′ and 31°13′ N (Fig. 1). North Sinai, as a desert region, has an arid climate with hot summer, mild winter, and an annual rainfall of 20–100 mm (Ayyad and Ghabour 1986). The topography comprises low alluvial plains, which are broken by large uplifted Mesozoic domes and anticlines. North of Gabel Maghara, the area extending near to the Mediterranean coast is a broad tract of sand dunes, some of which attain heights of 91 m above sea level (Said 1990). North Sinai is classified into three geomorphological districts: Mediterranean coastal district, anticlines district, and inland (transition) district. The Mediterranean coastal district extends 20–40 km southward from the Mediterranean coast. The open undulating sandy plains occupy most of the Mediterranean coastal district with coarse sand as the soil surface. Different types of sand dunes are prominent in the district. Salt marshes are located at depressions and near the foothills of sandy dunes (Hassan 2002).

Digital image processing

The following remote sensing analyses used data from the Landsat 7 ETM+ sensor (Level 1b data) dated to year 2005. The ETM+ data of the blue to the short-wave infrared portion of the spectrum were used in this study. Firstly, the thermal bands were excluded due to the nature of the study. The 30-m spatial resolution data in the visible/NIR bands were resampled to the higher 14-m resolution of the gray band. The image was georectified to UTM coordinates to be included into the exiting digital image and GIS database. All further digital image processing and analyses of Landsat 7 ETM+ satellite image were executed using the standard approaches provided by the software ENVI 4.6 (ITT 2008). The processing of data was represented by calibration to spectral radiance according to Lillesand and Kiefer (2007), where the calibration factors for each band were provided by (Chander et al. 2009). The Landsat ETM+ data were then atmospherically corrected using FLAASH module in ENVI 4.6 (ITT 2008).

The selection of appropriate end-members plays a vital role for determining pure signatures to representative homogeneous land covers from satellite sensor images (Rashed et al. 2003; Wu and Murray 2003). A minimum noise fraction (MNF) procedure described by Green et al. (1988) was employed to determine the inherent dimensionality of image data and to reduce the image data into a small number of significant bands suitable for end-member selection (Boardman and Kruse 1994; Boardman et al. 1995). According to the normalized eigenvalues >1, selected MNF components were

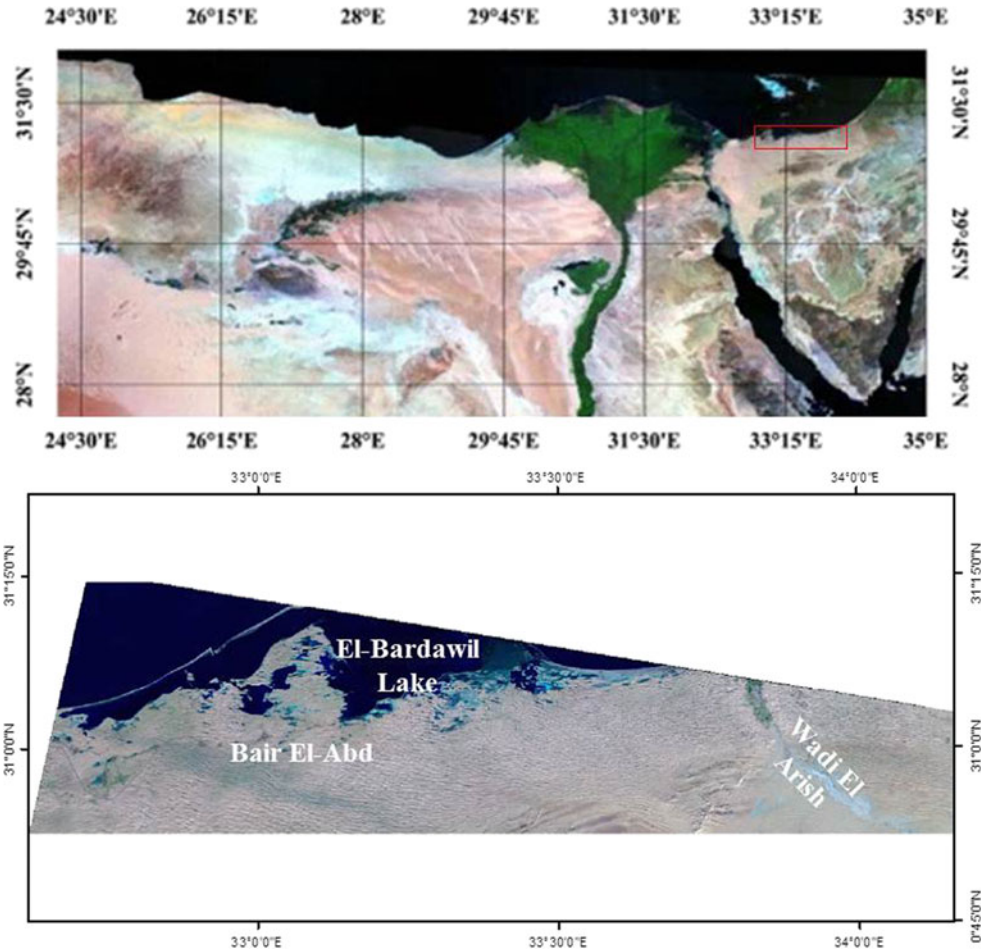

Fig. 1 Location map of the study area (false color composite 742 ETM+)

input to the pixel purity index (PPI) procedure to determine the purest pixels. The image-derived end-members, spectrally pure pixels, were identified by projecting the MNF and PPI results in an *n*-dimensional visualizer. The PPI image was geographically linked to the original image. A water mask was applied prior to the spectral unmixing to avoid the incorporation of related end-members. The final end-member used for spectral unmixing have been determined by a pixel purity analysis (PPI) that identifies the purest pixels on the edges of the multidimensional point cloud of pixel vectors. According to the PPI selected candidate pixel evaluation, four final end-members were selected to subsequently perform the field data collection.

Field data collection

Field spectra

Georeferenced spectral data for surface soil types were collected using ASD FieldSpec®3 portable spectroradiometer (ASD 2007) in a field campaign carried out in December 2010. FieldSpec acquires visible near-infrared and short-wave infrared spectra in the 0.35- to 2.50-μm spectral range. The spectral measurements were carried out within test plots representing a specific soil type. For each sample or surface, 100 consequent measurements using a pistol grip device yielded an average spectrum. Before and after the measurements, a white reference measurement has been taken. Reflectance spectra were obtained by comparing the radiance of the target with the radiance of a reference panel. Target and reference scans were made successively and compared to produce reflectance measurements.

Soil sampling

Fourteen soil profiles were dug for the identification of the different soil type characteristics represented in the study area. A soil profile was dug at each corresponding point after a spectral measurement was completed. Soil samples representing the subsequent variations within the soil horizons were collected for laboratory analyses of some chemical and physical soil properties. The soil profiles were dug to a depth of 150 cm, unless obstructed or hindered by bedrock. The soil samples were thoroughly examined and morphologically described in the selected sites according to the system outlined by FAO (2006).

Data analyses

Field spectra data

A set of processing operations should be performed before a thematic evaluation of data measured with an ASD field spectrometer. In order to prepare raw spectra measured with an ASD field spectrometer for further use, basic sequence of processing operations has to be performed. The collected raw spectra by the field spectrometer were imported into an ENVI spectral library and corrected for panel reflectance since the target reflectance was slightly overestimated. For any change in the radiation conditions, the white reference was checked and the spectra were interpolated. Any spectra containing measurement errors need to be removed as the erroneous spectra falsely influence the average spectra of the target. An indication for erroneous spectra can be peaks at unusual wavelengths or a spectrum that differs a lot from other spectra measured of the same target during the same measurement. The collected field spectra end-members corresponding to soil surface types were introduced into the linear spectral unmixing model to map the surface soils identified.

Remotely sensed image data

A linear spectral unmixing model was applied to the pre-processed multispectral data to determine pixel fractions of the four soil types:

$$\rho_{pixel} = \sum \{\rho_e \cdot c_e\} + \varepsilon = \left\{ \begin{array}{l} \rho_{st_1} \cdot c_{st_1} + \\ \rho_{st_2} \cdot c_{st_2} + \\ \rho_{st_3} \cdot c_{st_3} + \\ \rho_{st_4} \cdot c_{st_4} \end{array} \right\} + \varepsilon$$

$$\sum c_e = 1.0 \text{ and } 0 \leq c_e \leq 1.0$$

where p and C are the reflectance and surface fraction of each end-member (soil type, st), respectively, and ε is an error term.

The individual surface fractions sum to unity. The outputs of SMA are fractional surface images of input materials, which are scaled from 0 to 1.0. Zero indicates that none of the target material is present in the pixel, while 1 indicates complete cover. In addition to the fractional surface images, a root mean square error (RMSE) image is also produced. The RMSE image gives an indication of the degree to which the input end-members matched the extent of the materials on the ground.

Soil analyses

The soil samples obtained from the field which represent the soil types identified by spectral mixture analyses were collected, air-dried, crushed softly, and passed through a 2-mm sieve to get the "fine earth." The fine earth of soil samples was subjected to physical and chemical analyses, where particle size distribution was determined according to Bandyopadhyay (2007). Soil color (wet and dry) was identified with the aid of Munssel color charts (Soil Survey Staff 1951). Electric conductivity (EC, in deciSiemens per meter), soluble cations and anions, calcium carbonates ($CaCO_3$, in percent), organic matter (OM, percent), pH, exchangeable Na, and cation exchange capacity (CEC, in centimoles+ per kilogram) were determined according to Bandyopadhyay (2007).

Results and discussion

The MNF transformation explores the possible image end-members for this study. The first three components of MNF transformation were analyzed and described, with 77.67%, 17.00%, and 2.09% of the variability of all six ETM+ bands, respectively. The end-members were identified through the MNF component scatterplots. According to the MNF, PPI

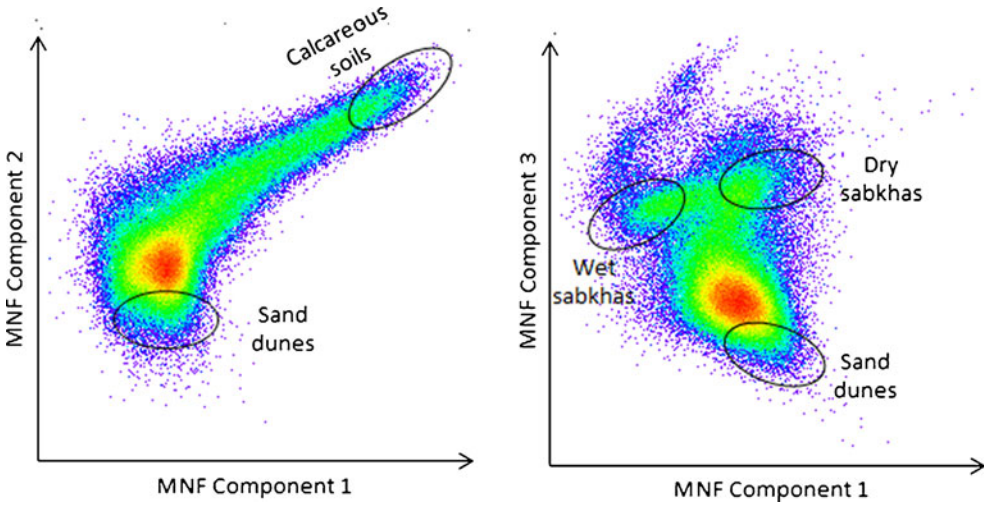

Fig. 2 Scatterplot of the first three MNF components (the *color* refers to the point density) with indicated feature spaces for main surface soil types of the study area (approximate locations)

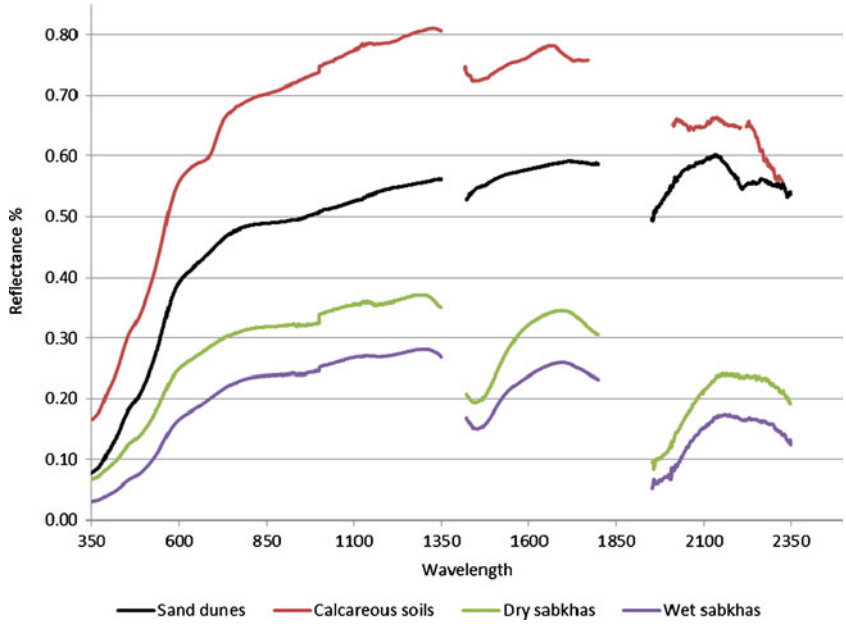

Fig. 3 Example field spectral reflectance of surface soil types collected. Water absorption bands ranging 1,360–1,400 nm and 1,800–1,980 nm were removed

results, and laboratory analyses, four main soil types dominating in the area were identified as end-members, which are calcareous soils, dry sabkhas, wet sabkhas, and sand dunes. The scatterplots shown in Fig. 2 indicate the information and spectral mixing situation of the dataset in the study area.

The scatterplots emphasize an end-member mixing situation. This is highlighted by the cloud of pixels as a spectral mix between these surface characteristics. Dry sabkhas and wet sabkhas have a large variability and overlap. This is due to their spectral similarity, hence will not accurately unmix, and the spectral mixture between these soil types can be separated into related end-member fractions during the linear spectral unmixing. The usual spectral mixing characteristics with pure pixels (one soil type) at the edges of the point cloud and mixed pixels in the center are represented in the scatterplots (Fig. 2). For example, MNF components 1 and 2 represent a large number of pixels appearing between the calcareous soils and sand dunes end-members. The fractions derived from these end-members were used to map the surface soil types in the study area.

Image spectra were established for each soil surface feature after confirming an appropriate match between field spectra and pixel spectra. The established spectra for each surface feature are shown in Fig. (3). The spectra represent the distinct surface soil type features. This can be distinguished according to their spectral reflectance property within the given range of the spectrum.

The diagnostic absorption features of soils are due to the inherent spectral behavior of the mineralogical composition, organic matter, and water (Baumgardner et al. 1985; Irons et al. 1989). The prominent absorption bands around the 1450- and 1,950-nm wavelength in most soil spectra are attributed to water and hydroxyl ions. Occasional weaker absorption bands caused by water also occur at 970, 1,200, and 1,770 nm. Absorption features near the 400-nm wavelength for all samples are also noticeable. The corrected soil type spectra were simulated to match the spectral response of ETM+ data (Fig. 4) using a Gaussian model with the provided wavelengths and the full width at half-maximum (FWHM) spacings. The simulated spectra (Fig. 5) represented to the linear unmixing model, and the spatial distributions of each soil surface features were mapped.

The characteristics of the different soil types identified in the study area and its associated classification according to

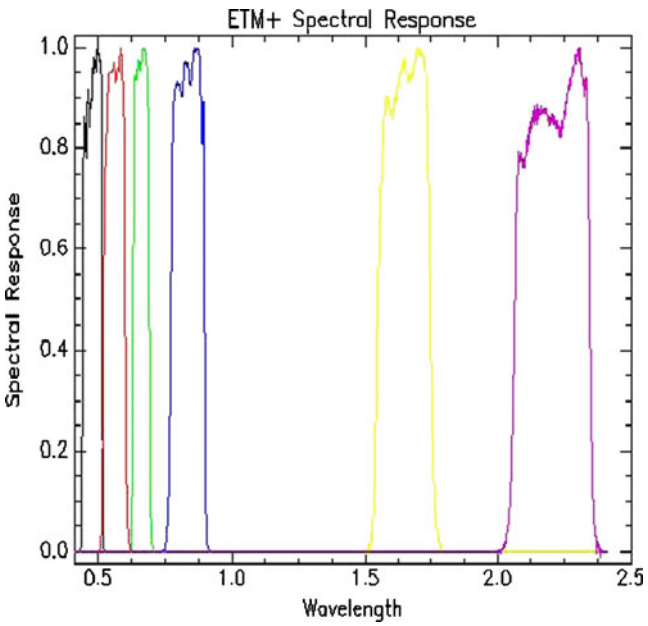

Fig. 4 ETM+ spectral response

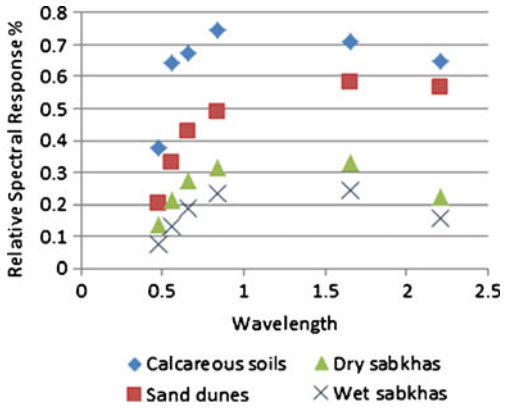

Fig. 5 Simulated surface soil types spectra

the Keys to Soil Taxonomy (USDA 2010) could be summarized as follows:

Sand dunes areas The mapped sand dunes surfaces (Fig. 6) occupy a considerable area especially in the southern part of Bair El-Abd area. They are generally arranged parallel to each other or sub-parallel to the resultant direction of the effective winds, where they follow a NW–SE direction and curve southward to follow an E–W direction. The parent material of these sand dunes is sandy deposits formed by the erosion of weathered surface materials transported and deposited by winds (Hola 2000). Some areas are covered with natural vegetations with few to common density of distribution. The soils of these sand dunes are non-saline and have low calcium carbonate content. The soil profile depth is more than 1.5 m. Saturation percentage lies around 22%. Soil texture class has the same pattern of sedimentation, where it is medium sand. These soils are almost free of soluble salts, whereas the EC values are very low as they lie around 0.7 dS/m, showing a seasonal leaching process by the considerable amounts of rain. Gypsum, $CaCO_3$, and OM contents are low, as well as the CEC in the successive soil horizons. The category of soil classification according to USDA soil taxonomy is *Typic Torripsamments*.

Sabkhas areas There are many dry sabkhas and wet sabkhas mapped in the study area. They are flat to almost flat surfaces occupying low-lying areas. The largest ones lie between El-Nigila and Rabaa. In addition, there are many sabkhas around the El-Bardawil Lake. These Sabkhas are restricted to the sandy flats that fringe the lake at the extreme eastern and western ends. The dune sabkha occupies most of the lake's southern shores, where the longitudinal sand ridges intersect the lake water (Hola 2000; Hassan 2002). The evaporation wavy surface of flat Sabkhas was identified at many locations in the Bair El-Abd and Rabaa area. The surface of sabkhas has a darker color than the surroundings and is composed mainly of magnesium (Mg) and sodium (Na) chlorides in addition to calcium sulfates ($CaSO_4$). The soil depth of these sabkhas ranges between 35 and 40 cm and limited by water table. The texture is coarse sand to clayey. These soils are highly affected by soluble salts which range between 21 and 125 dS/m. The calcium carbonate contents range between 0.3% and 36%, where the high values refer to shell fragments and fine segregations of $CaCO_3$. The gypsum content may reach 9%. CEC values range between 8 and 39 cmol+/kg soil. Soils of this unit could be classified as *Typic Aquisalids*, *Calcic Aquisalids*, and *Gypsic Haplosalids*.

Calcareous areas The majority of mapped calcareous soils are presented in Wadi El-Arish, whereas the main stream runs through several conspicuous steps facing the north and parallels the present shoreline which has an E–W direction in Wadi El-Arish area. The surface of these soils is flat to mainly almost flat, and some parts are undulating to rolling.

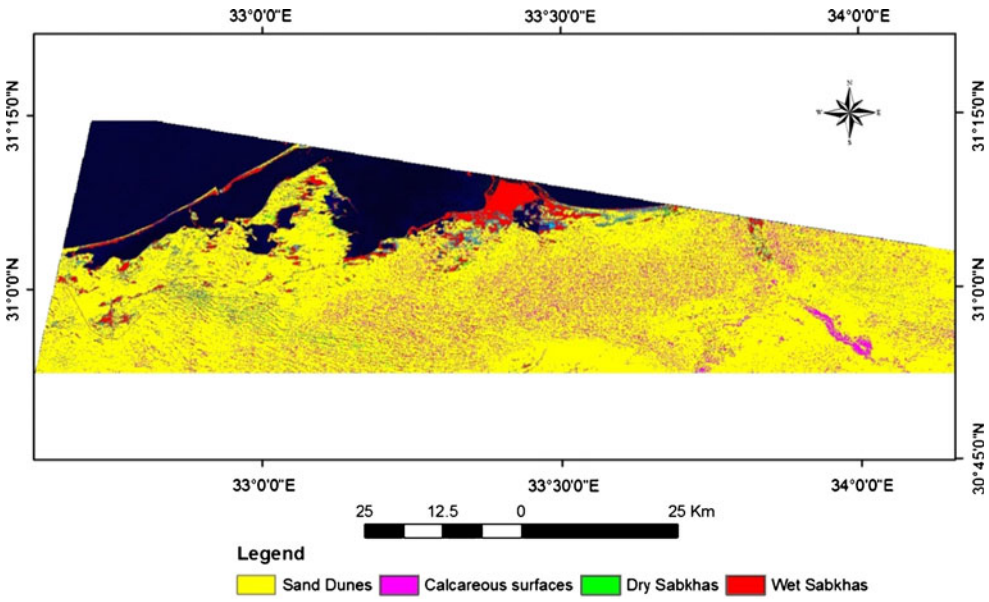

Fig. 6 Map of surface soil types using unmixing spectra model with field spectral data